Molecular Neurobiology (2019) 56:7810–7821
https://doi.org/10.1007/s12035-019-1633-z

Palbociclib Effectively Halts Proliferation but Fails to Induce Senescence in Patient-Derived Glioma Stem Cells

Olivia Morris-Hanon[1] · Mariela Claudia Marazita[1] · Leonardo Romorini[1] · Luciana Isaja[1] · Damián Darío Fernandez-Espinosa[1] · Gustavo Emilio Sevlever[1] · María Elida Scassa[1] · Guillermo Agustín Videla-Richardson[1]

Received: 22 January 2019 / Accepted: 2 May 2019 / Published online: 23 May 2019

Abstract

Glioblastoma multiforme is the most aggressive primary brain tumor. Current knowledge suggests that the growth and recurrence of these tumors are due in part to the therapy-resistant glioma stem cell subpopulation, which possesses the ability for self-renewal and proliferation, driving tumor progression. In many cancers, the $p16^{INK4a}$-CDK4/6-pRb pathway is disrupted in favor of cell cycle progression. In particular, the frequent deregulation of CDK4/6 in cancer positions these kinases as promising targets. Palbociclib, a potent and selective CDK4/6 inhibitor, has been approved by the FDA as a first-line treatment of advanced breast cancer and there is currently interest in evaluating its effect on other cancer types. Palbociclib has been reported to be efficient, not only at halting proliferation, but also at inducing senescence in different tumor types. In this study, we evaluated the effect of this inhibitor on four patient-derived glioma stem cell-enriched cell lines. We found that Palbociclib rapidly and effectively inhibits proliferation without affecting cell viability. We also established that in these cell lines CDK6 is the key interphase CDK for controlling cell cycle progression. Prolonged exposure to Palbociclib induced a senescent-like phenotype characterized by flattened morphology, cell cycle arrest, increased β-galactosidase activity and induction of other senescent-associated markers. However, we found that after Palbociclib removal cell lines resumed normal proliferation, which implies they conserved their replicative potential. As a whole, our results indicate that in patient-derived glioma stem cell-enriched cell lines, Palbociclib induces a senescent-like quiescence rather than true senescence.

Keywords CDK4/6 · Glioma stem cells · Palbociclib · Quiescence · Senescence

Introduction

Glioblastoma multiforme (GBM) is the most prevalent and malignant form of primary brain cancer. Even with aggressive combination therapies, the prognosis remains dismal with a median survival of 15 months after diagnosis [1]. Many tumors, including GBM, are hierarchically organized and sustained by a minor subpopulation of tumor cells called cancer stem cells (CSCs). Glioma stem cells (GSCs) share several essential features with neural stem cells, including self-renewal, the formation of neurospheres, expression of stem cell markers, differentiation potential, and localization to microenvironment niches [2–4]. Their ability to promote angiogenesis, tumor invasion and chemo-resistance renders GSCs a potential target for therapy in order to avoid GBM relapse.

Excessive cell proliferation induced by aberrant entry into the cell cycle is a common thread found in all forms of cancer [5]. Cell cycle progression is orchestrated by particular cyclin dependent kinases (CDKs) and their interaction with their regulatory cyclin partners [6, 7]. Whereas mitogenic stimuli induce cyclins and therefore activate CDKs, anti-mitogenic signals prevent cell cycle progression principally by inducing members of two families of CDK inhibitors (CKIs), the INK4 ($p16^{INK4a}$, $p15^{INK4b}$, $p18^{INK4c}$, and $p19^{INK4d}$) and the Cip/Kip ($p21^{Waf1}$, $p27^{Kip1}$, and $p57^{Kip2}$) families. While INK4 members specifically inhibit CDK4/6 catalytic activity, Cip/Kip

Electronic supplementary material The online version of this article (https://doi.org/10.1007/s12035-019-1633-z) contains supplementary material, which is available to authorized users.

✉ Guillermo Agustín Videla-Richardson
willyvidelar@hotmail.com

[1] Laboratorial de Investigación aplicada a Neurociencias (LIAN), Fundación para la Lucha contra las Enfermedades Neurológicas de la Infancia (FLENI), Ruta 9, Km 52.5, B1625XAF Buenos Aires, Argentina

members affect the activities of cyclin D-, E-, and A-dependent kinases complexes [8]. The uncontrolled proliferation of several human cancers is associated with the deregulation of CDKs, which frequently consists of aberrant expression of cyclins, CKIs, or CDKs. Cyclin D-CDK4/6 complexes phosphorylate and inactivate retinoblastoma (pRb) family proteins, leading to release of E2F transcription factors, which in turn promote progression of cells into the S phase of the cell-division cycle [9].

In many cancers, the $p16^{INK4a}$-CDK4/6-pRb pathway is commonly disrupted in favor of cell cycle progression and continued growth, rendering this pathway a key target for cancer therapeutics. Importantly, approximately 78% of GBM have defects in the $p16^{INK4a}$-CDK4/6-pRb pathway, including homozygous deletion of CDKN2A/2B (*p16*^{INK4a}/$p14^{ARF}$/$p15^{INK4b}$), amplification of CDK4/6 and deletion or mutation of pRb. These observations highlight the critical role of the $p16^{INK4a}$-CDK4/6-pRb pathway in GBM and suggest that targeting this pathway might be a promising strategy to improve the therapeutic efficacy [10].

Deregulation of CDK4/6 in cancer often leads to addiction to its activities, thus these kinases are emerging as particularly promising therapeutic targets. In this regard, Palbociclib (PD-0332991) was reported in 2004 as a potent and selective inhibitor of CDK4/6 with no appreciable activity against other kinases [11]. This inhibitor has been approved by the FDA in 2015 as a first-line treatment combined with endocrine therapy of advanced breast cancers [12, 13]. Palbociclib potently suppresses pRb phosphorylation and inhibit the proliferation of multiple tumor cells [11, 14]. Consistently, Palbociclib shows no anti-proliferative activity in pRb-deficient cell lines where the requirement for CDK4/6 is bypassed [15]. Notwithstanding, it has been shown that depending on the cell type and the transforming events, after sustained exposure to Palbociclib some pRb-proficient cells lines undergo quiescence and others undergo senescence [16–18]. Unlike quiescent cells, senescent cells irreversibly exit cell cycle and exhibit a flattened and enlarged morphology accompanied by an increased senescence-associated β-galactosidase (SA-β-gal) activity [19].

In the present study, we investigated the effect of impairing CDK activities in patient-derived glioma stem cell-enriched cell lines (GSC-ECLs) previously isolated and characterized in our laboratory. Importantly, these cell lines harbor homozygous deletions of the *CDKN2A/ARF* gene, which encodes $p16^{INK4a}$, a key player in the senescence program [4]. Firstly, we found that unlike CDK4 and CDK2, CDK6 has a major role in the proliferation of these cells. Then, we determined that the prolonged treatment of GSC-ECLs with Palbociclib led to cell cycle arrest and the appearance of senescence features such as enlarged flattened morphology, increased SA-β-gal activity and upregulation of senescence-associated secretory phenotype (SASP) molecules. However, when this inhibitor was withdrawn, cells resumed proliferation. As a whole, these results demonstrate that the action of this drug in patient-derived GSC-ECLs effectively inhibits cell proliferation but fails to induce cellular senescence.

Materials and Methods

Cell Culture and Treatments

Human fibroblasts (HF) were derived from freshly obtained foreskins and cultured in DMEM plus 10% fetal bovine serum as previously described [20]. GSC-ECLs, named G02, G07, G08, and G09, were isolated from human GBM biopsies and characterized as described in previous reports [4, 21]. Isolation of HF and GSC-ECLs from human biopsies was carried out accordingly to relevant guidelines and national regulations. The use of these cell lines for the experimental procedures included in this project has been authorized by the Biomedical Research Ethics Committee "Comité de Ética en Investigaciones Biomédicas de la Fundación para la Lucha contra Enfermedades Neurológicas de la Infancia (FLENI)". Written informed consent was received from patients whose samples were used. Neural progenitors (NP) were derived from human embryonic stem cells WA09 (cell line ID: WAe009-A) (WiCell Research Institute, Madison, WI, USA) [20]. GSC-ECLs and NP were cultured in serum-free conditions that comprise: Neurobasal medium supplemented with B27, N2, 20 ng/ml basic fibroblast growth factor (bFGF), 20 ng/ml epidermal growth factor (EGF) and plated onto Geltrex-coated plates (10 μg/ml). All cell culture reagents were obtained from Thermo Scientific, Rockford, IL, USA.

Palbociclib, Roscovitine, GSK690693, and Rapamycin were purchased from Sigma St. Louis, MO, USA. For hydrogen peroxide (H_2O_2) (Merk, Kenilworth, NJ, USA) treatments, cells were exposed to either 150 μM (GSC-ECLs) or 90 μM (HF) of H_2O_2 for 1 h on 3 consecutive days, after which cells were cultured in the appropriate fresh medium for 11 days before experimental determinations.

Reverse Transcription Polymerase Chain Reaction

RNA extractions were carried out using TRIzol reagent (Thermo Scientific, Rockford, IL, USA) according to manufacturer's instructions. cDNA synthesis was performed using the MMLV reverse transcriptase (Promega, Madison, WI, USA). Quantitative RT-PCR assays were conducted using SYBR® Green-ER™ qPCR SuperMix Universal (Thermo Scientific, Rockford, IL, USA). Primer sequences: CDK2 forward 5′-CCCTTTCTTCCAGGATGTGA-3′, reverse 5′-TGAGTCCAAATAGCCCAAGG-3′; CDK4 forward 5′-TGCAACACCTGTGGACATGTG-3′, reverse 5-′ ATTTGCCCAACTGGTCGG-3′; CDK6 forward 5′-TCCC

TCCTTTGAAGTGGATG-3′, reverse 5′-GTCA CCTGGGGCTAAATGAA-3′; IL-6 forward 5′-CCTG AACCTTCCAAAGATGGC-3′, reverse 5′-TTCA CCAGGCAAGTCTCCTCA-3′; IL-8 forward 5′-ACTG AGAGTGATTGAGAGTGGAC-3′, reverse 5′-AACC CTCTGCACCCAGTTTTC-3′; PAI-1 forward 5′-ACCG CAACGTGGTTTTCTCA-3′, reverse 5′-TTGA ATCCCATAGCTGCTTGAAT-3′; bFGF forward 5′-AGAG CGACCCTCACATCAAG-3′, reverse 5′-GCCA GTAATCTTCCATCTTCCTTC-3′; EGF forward 5′-CATC GTGGTGGCTGTCTG-3′, reverse 5′-GCTT CTGAGTCCTGTAGTAGTG-3′; RPL7 forward 5′-AATG GCGAGGATGGCAAG-3′; reverse 5′-TGAC GAAGGCGAAGAAGC-3 VEGF forward 5′-CATC TTCAAGCCATCCTGTGTG-3′, reverse 5′-CCGC ATAATCTGCATGGTGAT-3′.

Western Blotting

Cells were lysed in radio immunoprecipitation assay (RIPA) buffer supplemented with a protease inhibitor mixture. Protein concentration was determined using Bicinchoninic Acid Protein Assay (Pierce™, Rockford, IL, USA). Immunoblotting was done as previously described [21]. The following primary antibodies were used: α-Actin (C-2) (sc-8432); α-CDK2 (M2) (sc-163); α-CDK4 (H-22) (sc-601); α-CDK6 (C-21) (sc-177) all from Santa Cruz Biotechnology, CA, USA. IR-Dye labeled secondary antibodies were used to detect antigen/primary antibody complexes (LI-COR Biosciences, Lincoln, NE, USA).

Cell Viability Assay (Trypan Blue Staining)

Cellular suspensions were mixed with a trypan blue solution (0.4%) at a 1:5 ratio and incubated for 5 min. Cells were analyzed in a hemocytometer without delay. Results were expressed as the percentage of cells that displayed trypan blue staining (non-viable) of the total number of cells processed.

Flow Cytometric Analysis of BrdU Incorporation and Cell Cycle Distribution

BrdU Flow Kit (BD Biosciences, San Jose, USA) was used to determine the fraction of cells capable of incorporating BrdU and characterize the distribution of cells throughout the cell cycle phases. After treatments, cells were exposed to BrdU (10 μM) for 2 h. Cells were then processed according to manufacturer's instructions and analyzed on a BD Accuri C6 flow cytometer (BD Biosciences, San Jose, USA) using the BD AccuriC6 software.

Cell Transfection and RNA Interference

Cells were transfected with small interfering RNA (siRNA) using Lipofectamine RNAiMAX (Thermo Scientific, Rockford, IL, USA) according to manufacturer's instructions. 2.5×10^5 cells/well (6-well plate) were transfected with silencer select negative control #2 (cat#4390846); CDK2 siRNA (ID: s205); CDK4 siRNA (ID: s2822); CDK6 siRNA (ID: s51). All siRNAs were obtained from Thermo Scientific, Rockford, IL, USA. Final concentrations of siRNA ranged between 2.5 and 5 nM. The corresponding assays were performed between 24 and 48 h after transfection.

Immunostaining and Fluorescence Microscopy

Immunostainings were performed as described in a previous report [21]. In brief, cells were fixed in a 4% formaldehyde solution for 15 min. Then, fixed cells were rinsed and permeabilized with 0.1% Triton X-100 in PBS plus 0.1% bovine serum albumin plus 10% fetal bovine serum for 30 min. Finally, cells were incubated overnight with the primary antibody in permeabilization buffer. Fluorescent-dye conjugated secondary antibodies (Thermo Scientific, Rockford, IL, USA) were used to detect the antigen/antibody complexes. Nuclei were stained with DAPI. Immunostained cells were examined under a Nikon Eclipse TE2000S microscope and images were obtained with a Nikon DXN1200F digital camera controlled by software EclipseNet version 1.20.0 build 61. Primary antibodies used α-Ki67 (NCL-Ki67-MM1) (Novocastra Laboratories, Newcastle, UK) and α-GFAP (AB5804) (Millipore, Billerica, MA, USA).

SA-β-Gal Staining

Cells were washed in PBS, fixed for 3–5 min in 4% formaldehyde, washed and incubated at 37 °C (no CO_2) with SA-β-Gal stain solution: 1 mg/ml of 5-bromo- 4-chloro-3-indolyl β-D-galactoside (X-Gal) (Promega, Madison, WI, USA), 40 mM citric acid/sodium phosphate (pH 6.0), 5 mM potassium ferrocyanide, 5 mM potassium ferricyanide, 150 mM NaCl, 2 mM $MgCl_2$. Staining was evident in 12–16 h. Fixed cells were examined under a Nikon Eclipse TE2000S microscope and images were obtained with a Nikon DXN1200F digital camera controlled by software EclipseNet version 1.20.0 build 61.

Growth Rate Estimation

Cells were plated at low density (3×10^4 cells per well in 24 well plates) in order to minimize the effect of density on cell growth, and treated as indicated in figure legends. After treatment cells were allowed to re-grow in fresh medium. On indicated days, cells were fixed, stained with DAPI and nuclei

were quantified to determine daily growth rate (percentage of population growth per day) using a standard growth rate formula.

Results

CDK4/6 Inhibition Induces Cell Cycle Arrest in GSC-ECLs

Initially, we examined the mRNA expression levels of CDK2, CDK4, and CDK6 in four GSC-ECLs and two non-tumor cell lines used as reference; HF as non-neural cells and NP as untransformed neural cells. In the case of CDK2 and CDK4 expression, real-time RT-PCR analysis revealed slight differences (although in some cases significant) between GSC-ECLs and non-tumor cell lines (HF and NP). However, CDK6 mRNA expression levels were markedly higher in GSC-ECLs than those detected in HF and NP (Fig. 1a). Western blot analysis showed reduced expression levels of CDKs in HF when compared with the rest of the cell lines. Importantly, as with mRNA levels, protein levels of CDK6 were markedly higher in GSC-ECLs than in the non-tumor cell lines (Fig. 1b). We also examined the CDK transcriptional pattern of HF, NP, and GSC-ECLs. In all studied cell lines, CDK2 was found to be the less expressed interphase CDK. However, the relative expression levels of CDK4 and CDK6 varied among cell types. In HF and NP, CDK4 resulted in the most abundant interphase CDK. On the other hand, in four GSC-ECLs, the most abundant CDK was by far CDK6 (Fig. 1c).

Then, we decided to explore the consequences of attenuating the CDK activities in NP and GSC-ECLs. To address this issue, we used Palbociclib, a specific CDK4/6 kinase inhibitor, and Roscovitine, a broad-range purine inhibitor that preferentially targets CDK1, CDK2, CDK5, and CDK7 [22, 23]. Initially, we evaluated the effect of these inhibitors on NP and GSC-ECLs viability. To do so, we performed a dose-response viability curve after 14 days of the corresponding treatments. Palbociclib and Roscovitine significantly affected NP and GSC-ECLs viability only when used at concentrations of 10 μM and 20 μM (or higher) respectively (Fig. 2a). Then, to elucidate whether non-toxic concentrations of these CDK inhibitors (Palbociclib 1 μM and Roscovitine 10 μM) cause changes in cell proliferation, we measured BrdU incorporation after 48 h of CDK inhibitors exposure. In all tested cell lines, Palbociclib strongly inhibited BrdU incorporation, while Roscovitine only led to partial inhibition of cell proliferation (Fig. 2b).

CDK6 Mainly Governs Proliferation of GSC-ECLs

We next used siRNA-mediated gene silencing to further dissect the individual contributions of CDK2, CDK4, and CDK6 in NP and GSC-ECLs proliferation (Fig. 3a). We found that in NP single downregulation of these CDKs did not affect cell proliferation, while simultaneous silencing of CDK4 and CDK6 significantly decreased the percentage of cells in S phase (Fig. 3b). As in NP, in GSC-ECLs CDK2 or CDK4 downregulation was insufficient to affect proliferation of GSC-ECLs. However, siRNA-mediated silencing of CDK6 led to a significant decrease in the proportion of $BrdU^+$ cells. Of note, simultaneous downregulation of CDK4 and CDK6 caused an effect similar to the one observed using only CDK6-specific siRNA (Fig. 3b). These results indicate that GSC-ECL proliferation is particularly reliant on CDK6 catalytic activity. In this regard, the fact that the expression of CDK6 is significantly higher in GSC-ECLs than in NP supports this finding (Fig. 1).

Sustained Palbociclib Treatment Induces a Senescent-like Phenotype in GSC-ECLs

Recent reports have shown that prolonged exposure to Palbociclib can induce senescence in some cancer cells [16, 18, 24]. Bearing this in mind, we sought to determine if this is the case in GSC-ECLs. Firstly, by immunostaining of glial fibrillary acidic protein (GFAP), an intermediate filament protein marker of astroglial cells, we explored whether treatments with Palbociclib or Roscovitine for 14 days affects the cellular morphology of GSC-ECLs. We found that prolonged exposure of GSC-ECLs to Palbociclib led to the appearance of enlarged and flattened cytoplasms, reminiscent of senescent cells (Fig. 4a). Then, to evaluate the effect of sustained exposure to Palbociclib or Roscovitine in cell proliferation, we determined Ki67 expression by immunostaining. We found that a 14-day treatment with Palbociclib provokes cell cycle exit in GSC-ECLs (Fig. 4b). Finally, we determined that the vast majority of Palbociclib-treated cells were positive for SA-β-gal staining (blue-green), a distinctive hallmark of cellular senescence (Fig. 4c). This SA-β-gal staining was also observed in the rest of studied cell lines (Suppl. Fig. 1). Therefore, extended Palbociclib treatment not only causes a sustained growth arrest but also induces senescent features. On the contrary, inhibition of CDKs by Roscovitine does not promote this senescent-like phenotype in GSC-ECLs (Fig. 4a–c).

It has been reported that pharmacological inhibition of mechanistic target of rapamycin (mTOR) suppresses the acquisition of the senescent-like phenotype triggered by CDK4/6 inhibition [18]. Thus, we sought to determine whether signaling through the protein kinase B (PKB)/mTOR pathway is involved in the induction of the observed senescent-like phenotype. To this end, we treated cells with specific inhibitors of PKB or mTOR (GSK690693 and Rapamycin respectively), both in the presence or absence of Palbociclib for 14 days. As seen in Fig. 4 d, exposure of GSC-ECLs to GSK690693 or Rapamycin led to the appearance of cells showing enlarged cell bodies but did not induce the expression of β-gal activity.

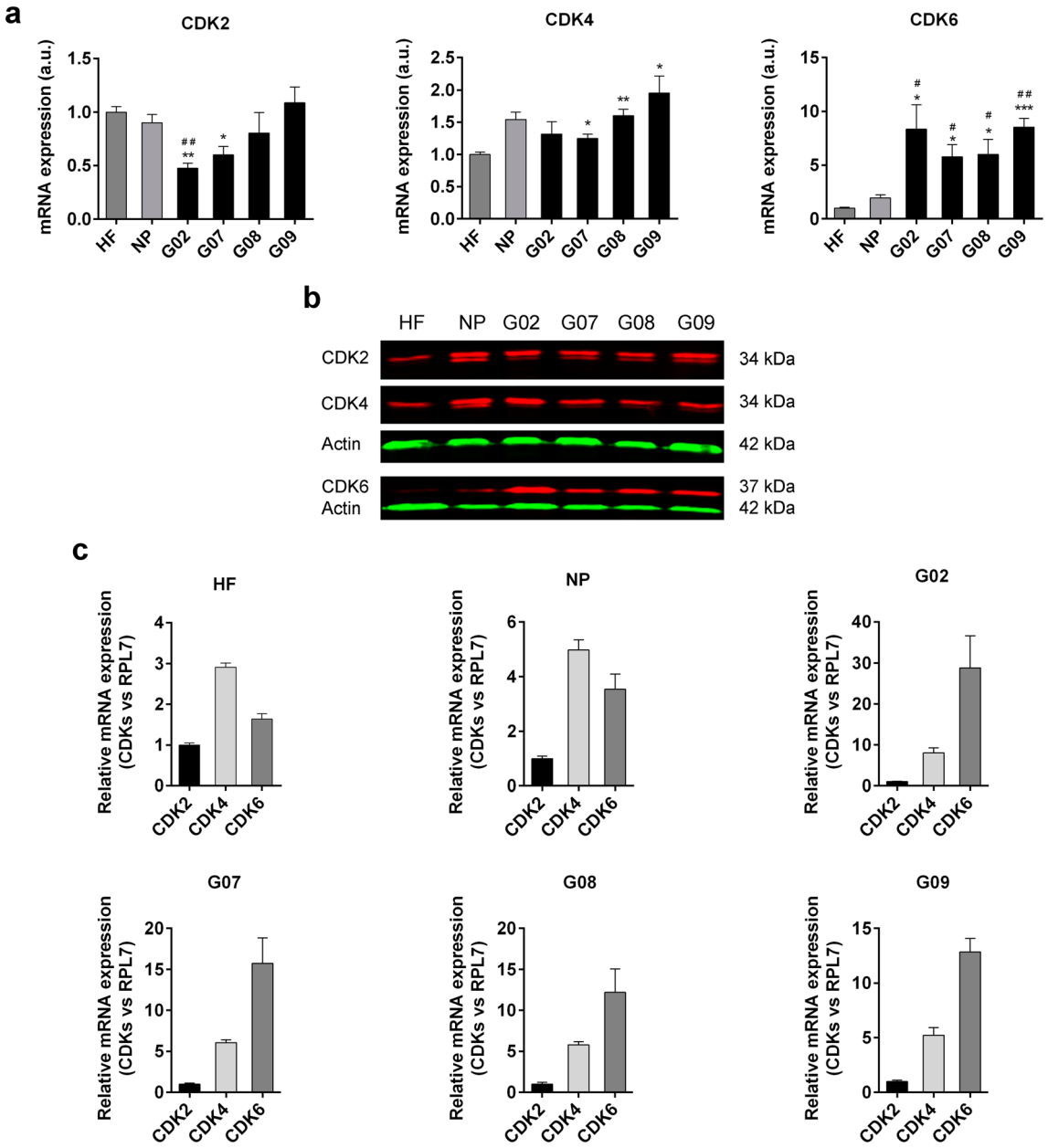

Fig. 1 Interphase CDK expression in HF, NP and GSC-ECLs. **a** mRNA expression levels of *cdk2*, *cdk4*, and *cdk6* were analyzed by RT-qPCR. Graph shows mRNA expression fold change relative to HF. Each bar represents the mean ± S.E.M. of three independent experiments. A Student's *t* test was used to detect significant differences between HF (*) or NP (#) and each GSC-ECL. $*P < 0.05$, $**P < 0.001$, $***P < 0.0001$. a.u.: arbitrary units. **b** Western blot analysis showing CDKs expression levels. Actin was used as loading control. **c** Transcriptional profile of CDKs by RT-qPCR. Results represent mRNA expression levels of each CDK relative to the corresponding RPL7 mRNA expression levels. Each bar represents the mean ± S.E.M. of three independent experiments

Moreover, we found that these inhibitors effectively suppressed the SA-β-gal$^+$ phenotype induced by Palbociclib (Fig. 4d and Suppl. Fig. 2).

Prolonged Exposure to Palbociclib Induces a SASP in GSC-ECLs

A combination of several different features is necessary to confirm the existence of cellular senescence. Thus, at this point of our study, we still need to conduct additional assays to evaluate whether Palbociclib induces senescence in GSC-ECLs. In order to set up a reference model, we utilized a widely accepted protocol for inducing senescence consisting of exposing HF to H_2O_2 [25]. As expected, H_2O_2 treatment caused a marked increase in SA-β-gal activity in both HF and GSC-ECLs (Suppl. Fig. 3). Thus, in the subsequent experiments, we used this H_2O_2-based protocol as a reference of senescence.

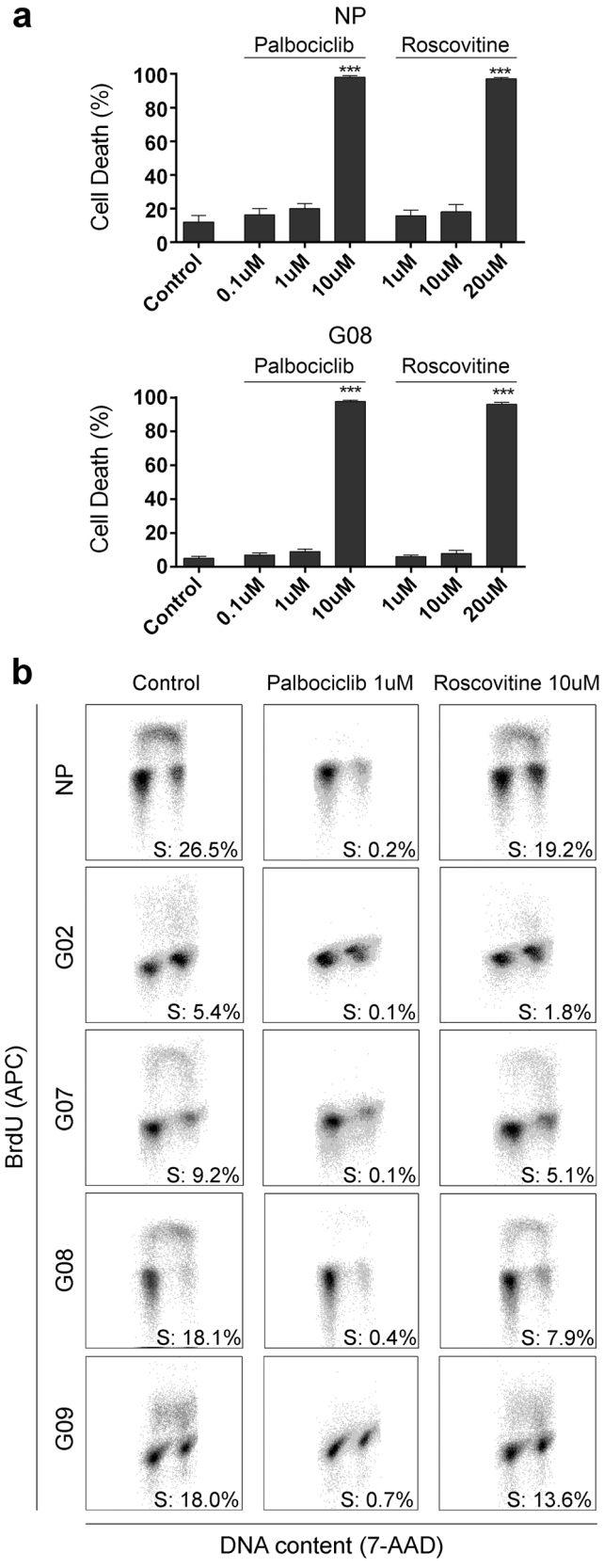

Fig. 2 Effect of Palbociclib and Roscovitine on cell death and cell cycle progression in NP and GSC-ECL. **a** Cell viability was measured by trypan blue staining in NP and G08 cells after a 14-day treatment with increasing concentrations of Palbociclib or Roscovitine. Results represent the percentage of cell death in each condition. The data express the mean ± S.E.M. of three independent experiments. A Student's *t* test was used to compare inhibitor-treated cells to untreated controls. ***$P < 0.0001$. **b** Cells were treated or not with Palbociclib or Roscovitine during 48 h. Cells were pulse-labeled with BrdU for 2 h, harvested, and stained with an anti-BrdU APC-conjugated antibody and with 7-amino-actinomycin D (7-AAD) for determination of DNA synthesis and DNA content respectively. A representative flow cytometry plot is shown for each experimental condition. The percentage of cells in S phase was determined by quantifying $BrdU^+$ events

One of the characteristics associated with senescence is the presence of a SASP, which is characterized by an increase in the expression of several factors involved in signaling pathways [26]. Even though cytokines, chemokines, and growth factors are defining components of the SASP, they can vary depending on the tissue, cell type, and stimulus used to induce senescence. Bearing this in mind, we examined the expression levels of six molecules known to be upregulated in the SASP: interleukin-6 (IL-6), interleuquin-8 (IL-8), plasminogen activator inhibitor-1 (PAI-1), bFGF, EGF, and vascular endothelial growth factor (VEGF). Initially, we analyzed the expression levels of these factors in H_2O_2-treated HF and found that they were all upregulated with the exception of EGF. This was not surprising as EGF is expressed mainly in epidermal tissues. When analyzing GSC-ECLs, we observed that both in H_2O_2- and Palbociclib-treated cells, the three growth factors (bFGF, EGF and VEGF) were significantly induced (Fig. 5). In the case of PAI-1 expression, although only H_2O_2 treatment caused a significant increase, Palbociclib exposure also showed a similar trend. Notably, IL-6 and IL-8 exhibited a cell line-specific behavior. While in G09 cell line both interleukins were upregulated in both treatments, in G08 cell line no significant changes were observed. These differences can be explained, at least in part, by the high inter-tumor heterogeneity described in GBM.

Palbociclib Treatment Does Not Eliminate Replicative Potential of GSC-ECLs

In spite of the fact that many cellular features are used as markers of senescence, the defining characteristic of this process consists in irreversible cell cycle exit. Considering this, we decided to evaluate the replicative potential by measuring growth rate and Ki67 expression in GSC-ECLs after a 14-day treatment with Palbociclib. Additionally, given that Rapamycin was able to suppress the Palbociclib-induced $SA\text{-}\beta\text{-}gal^+$ phenotype, we also evaluated the replicative potential after 14 days of Rapamycin, and a combination

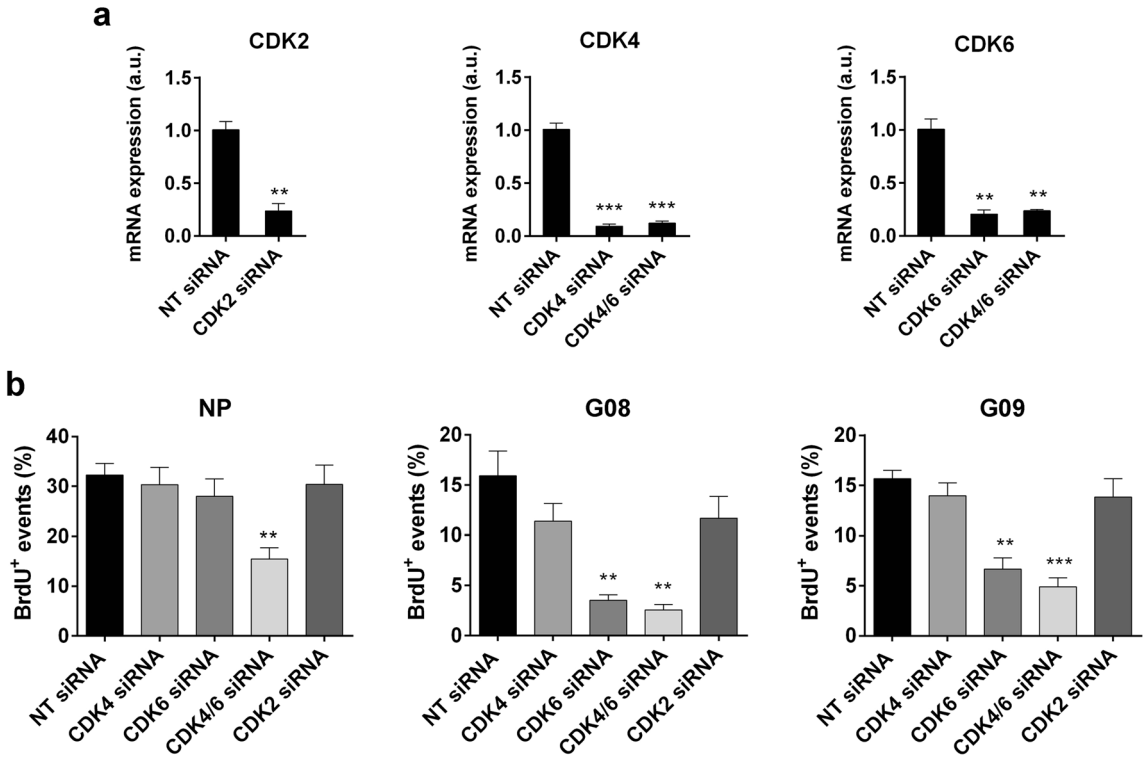

Fig. 3 CDK6 is a key regulator of GSC-ECL proliferation. **a** mRNA expression levels of *cdk2*, *cdk4*, or *cdk6* of single- or double-siRNA transfected cells were analyzed by RT-qPCR 24 h post-transfection. *rpl7* expression was used as normalizer. Graphs show mRNA expression fold change relative to non-targeting (NT) siRNA transfectants. Each bar represents the mean ± S.E.M. of three independent experiments. A Student's *t* test was used to detect significant differences. $^{**}P < 0.001$, $^{***}P < 0.0001$. a.u.: arbitrary units. **b** Cells were transfected with NT-siRNA or specific CDK-siRNAs as indicated in the figure and BrdU incorporation was evaluated 36 h post-transfection. Graphs show the percentage of $BrdU^+$ cells. Each bar represents the mean ± S.E.M. of three independent experiments. A Student's *t* test was used to detect significant differences of BrdU incorporation between CDK- and NT-siRNA transfectants. $^{**}P < 0.01$, $^{***}P < 0.001$

treatment of Palbociclib plus Rapamycin. Finally, just as in previous experiments, we included treatments with H_2O_2 as a reference, both in HF and in GSC-ECLs.

As expected, in H_2O_2-treated HF, we observed a permanent cell cycle arrest, marked by an almost complete reduction of cellular growth and a drastically diminished Ki67 staining. This behavior was also observed in GSC-ECLs exposed to H_2O_2 (Fig. 6). However, after treatment with Palbociclib, arrested GSC-ECLs recovered normal growth rate and Ki67 expression after between a 7 and 14 days lag period, indicating that replicative potential was conserved. This behavior was observed not only in G08 and G09 but also in the remaining tested GSC-ECLs (Suppl. Fig. 4). After the combined treatment of Palbociclib and Rapamycin, cells also recovered their growth rate and expression of Ki67; however, they did it later than the cells treated with Palbociclib alone. This result was somehow unexpected as Rapamycin suppresses the Palbociclib-induced senescent-like phenotype (Fig. 4d and Suppl. Fig. 2). In the presence of only Rapamycin, for 14 days, GSC-ECLs halted their proliferation and, after drug removal, resumed normal growth rate with kinetics similar with Palbociclib-treated cells. These results indicate that Palbociclib-and Rapamycin-treated cells stop proliferation but, unlike H_2O_2-treated cells, preserve their replicative potential.

Discussion

GBM frequently harbor genetic alterations that cause aberrant activation of cyclin D-CDK4/6 complexes [10]. Hence, it appears that direct inhibition of CDK4/6 activity results in a promising strategy to treat cancers.

In this study, we analyzed the inhibitory effect of Palbociclib on GSC-ECLs. We found that Palbociclib significantly suppresses proliferation of all tested cell lines. Importantly, we determined that knockdown of CDK6, but not of CDK4, mimicks the effects of Palbociclib on cell growth. This finding suggests that CDK6 is a major player in cell cycle progression in GSC-ECLs. In fact, it has been shown that CDK6 is over-expressed in hematopoietic malignancies, gliomas, and other several cancer types. [27]. Interestingly, herein, we found that all studied GSC-ECLs exhibit significantly higher levels of CDK6 than NP and HF.

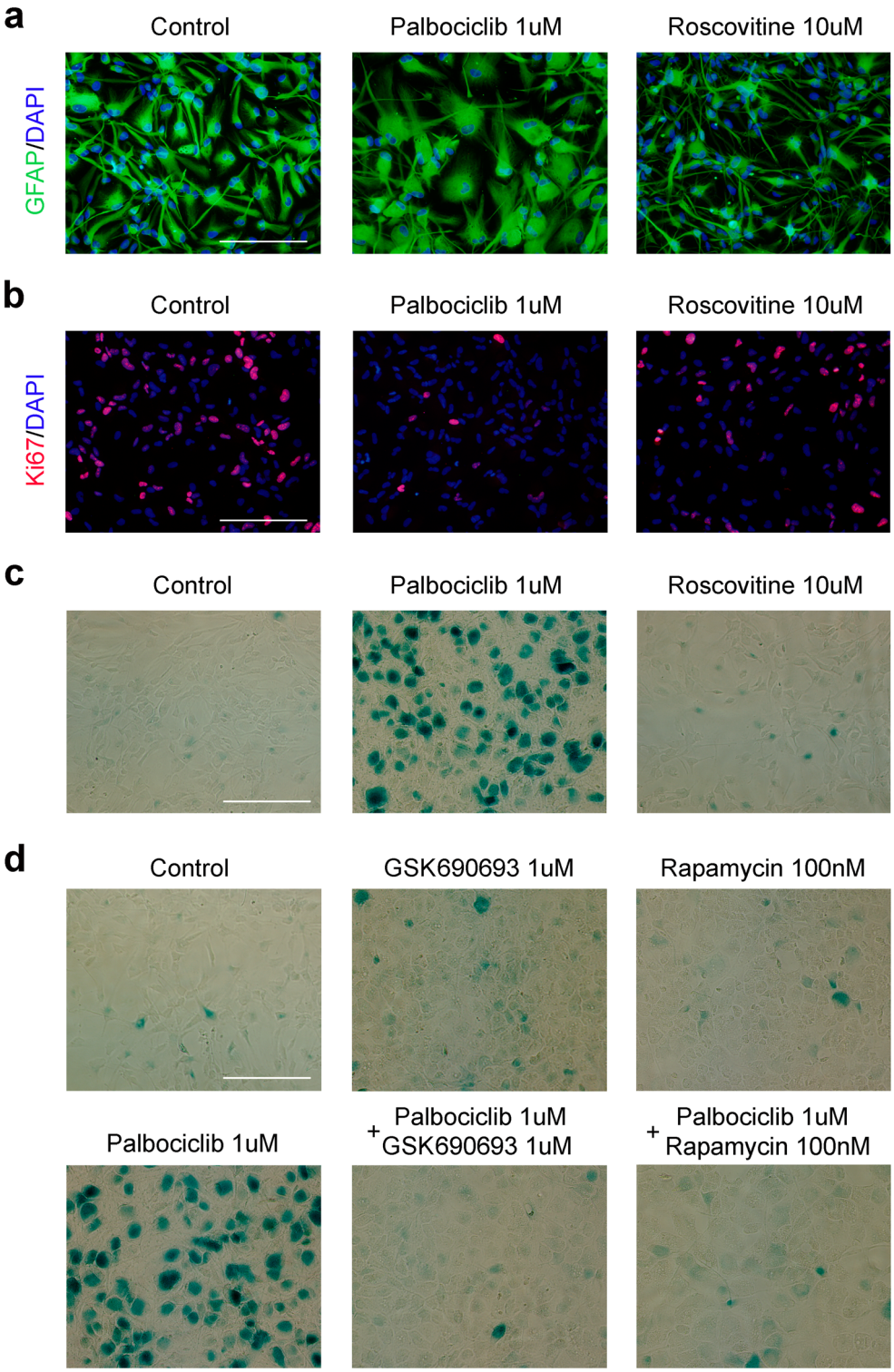

Fig. 4 Palbociclib induces a senescent-like phenotype in G08 GSC-ECL (**a** and **b**). Immunofluorescent images of cells treated or not with Palbociclib or Roscovitine for 14 days. Cells were stained with anti-GFAP and anti-Ki67 antibodies respectively. Nuclei were counterstained with DAPI (**c** and **d**). Inhibition of the PKB/mTOR signaling pathway impairs the Palbociclib-induced β-gal^{+} phenotype. Representative images of G08 cells treated or not with the indicated inhibitors for 14 days and stained for β-gal activity. Scale bar: 50 μm

Prolonged exposure to Palbociclib has been reported to induce a SA-β-gal phenotype in a wide range of cell types. On the other hand, it has been proved that Rapamycin inhibits senescence in human fibroblasts [28]. However, Rapamycin exerts opposing effects on different types of cancer cells. mTOR inhibitors have been shown to be effective against radio-resistant cancer cells by inducing a senescent-like growth arrest [29]. Moreover, Yoshida et al. observed that inhibition of mTOR signaling by Rapamycin cooperates with Palbociclib to induce senescence in melanoma cells [30]. However, this synergism appears to be cell-type specific as in the same study researchers found that Rapamycin exposure

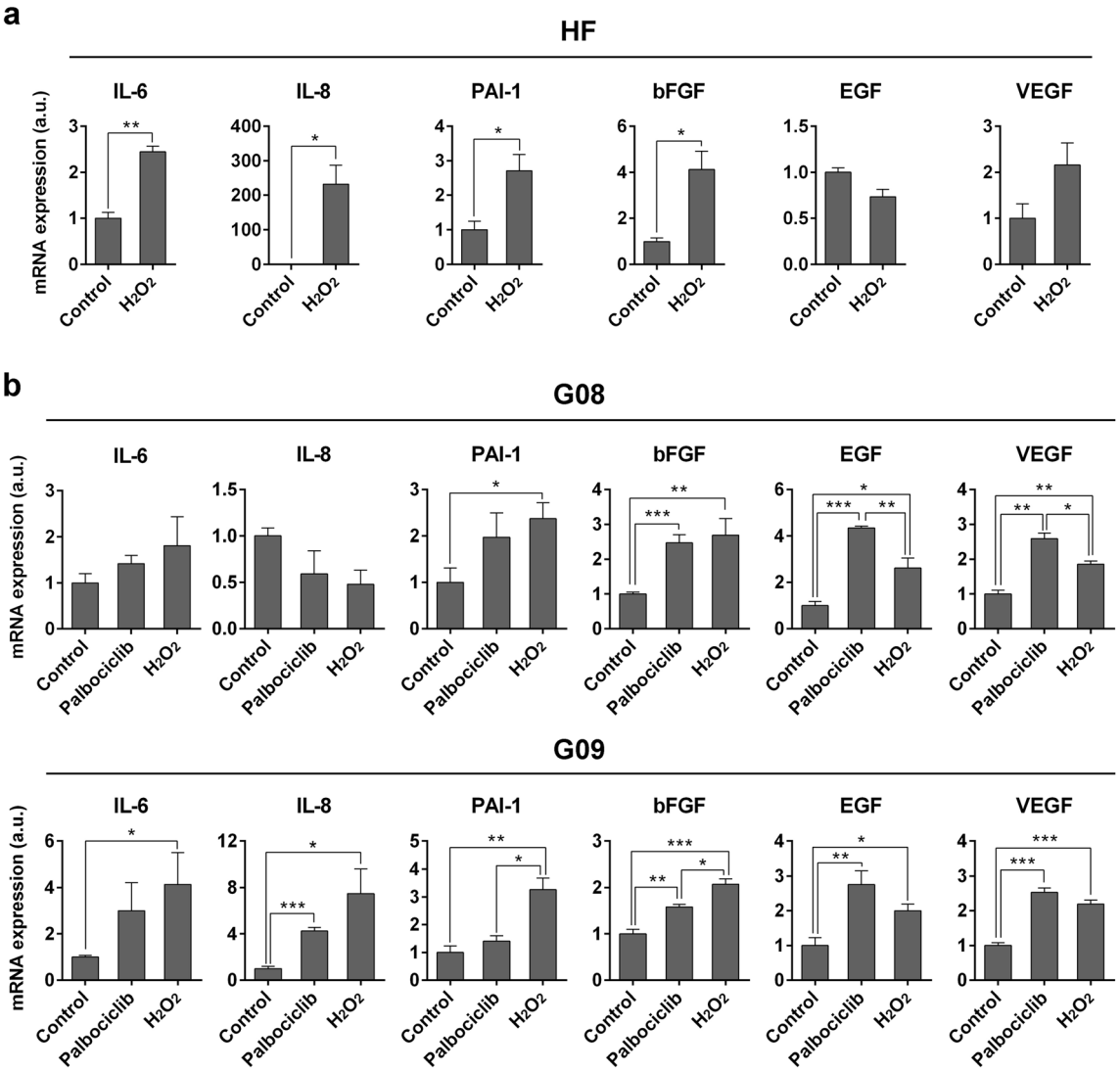

Fig. 5 Palbociclib induces a senescent-associated secretory phenotype in GSC-ECLs. mRNA expression levels of different components of the SASP were analyzed by RT-qPCR in HF and GSC-ECLs after a 14 day-exposure to Palbociclib or an H_2O_2 treatment (described in "Materials and Methods"). Graph shows mRNA expression fold change relative to control (untreated) cells. Each bar represents the mean ± S.E.M. of three independent experiments. A Student's *t* test was used to detect significant differences. $^*P < 0.05$, $^{**}P < 0.001$, and $^{***}P < 0.0001$ a.u.: arbitrary units

reverted Palbociclib-induced senescence in esophageal cancer cell lines. Given these diverse responses, we were prompted to explore the effect of Rapamycin in Palbociclib-treated GSC-ESCs and found that this mTOR inhibitor considerably impaired the appearance of SA-β-gal activity.

Numerous studies have shown that inhibition of CDK4/6 can induce either cellular quiescence or senescence, depending on the tumor cell type [16, 18, 31, 32]. In fact, it has been reported that Palbociclib can induce senescence in a wide range of glioma cell lines [17]. However, in this publication, the claim of senescence relies only on SA-β-gal activity. For this reason, we decided to evaluate if after prolonged exposure to Palbociclib GSC-ECLs also exhibit a SASP. We found that Palbociclib- or H_20_2-treated GSC-ECLs activate a SASP-like program that includes up-regulation of bFGF, EGF and VEGF which, within the tumor microenvironment, may help to maintain stemness, proliferation, and induce angiogenesis respectively. Moreover, H_20_2 led to a marked increase of PAI-1, which is associated with a shorter overall survival in patients with GBM [33]. We also determined that in G09 cell line IL-6 and IL-8, which are considered key regulators of glioma cell growth and invasiveness, were induced [34]. Therefore, the activation of a SASP, regardless of the attainment of true senescence, may promote tumor progression.

Given that the defining feature of senescent cells is the loss of proliferative potential, we evaluated whether these cells have effectively acquired an irreversible growth arrest. We measured cell growth after Palbociclib treatment and determined that GCS-ECLs recover their proliferative capacity within 21 days. These results indicate that Palbociclib-

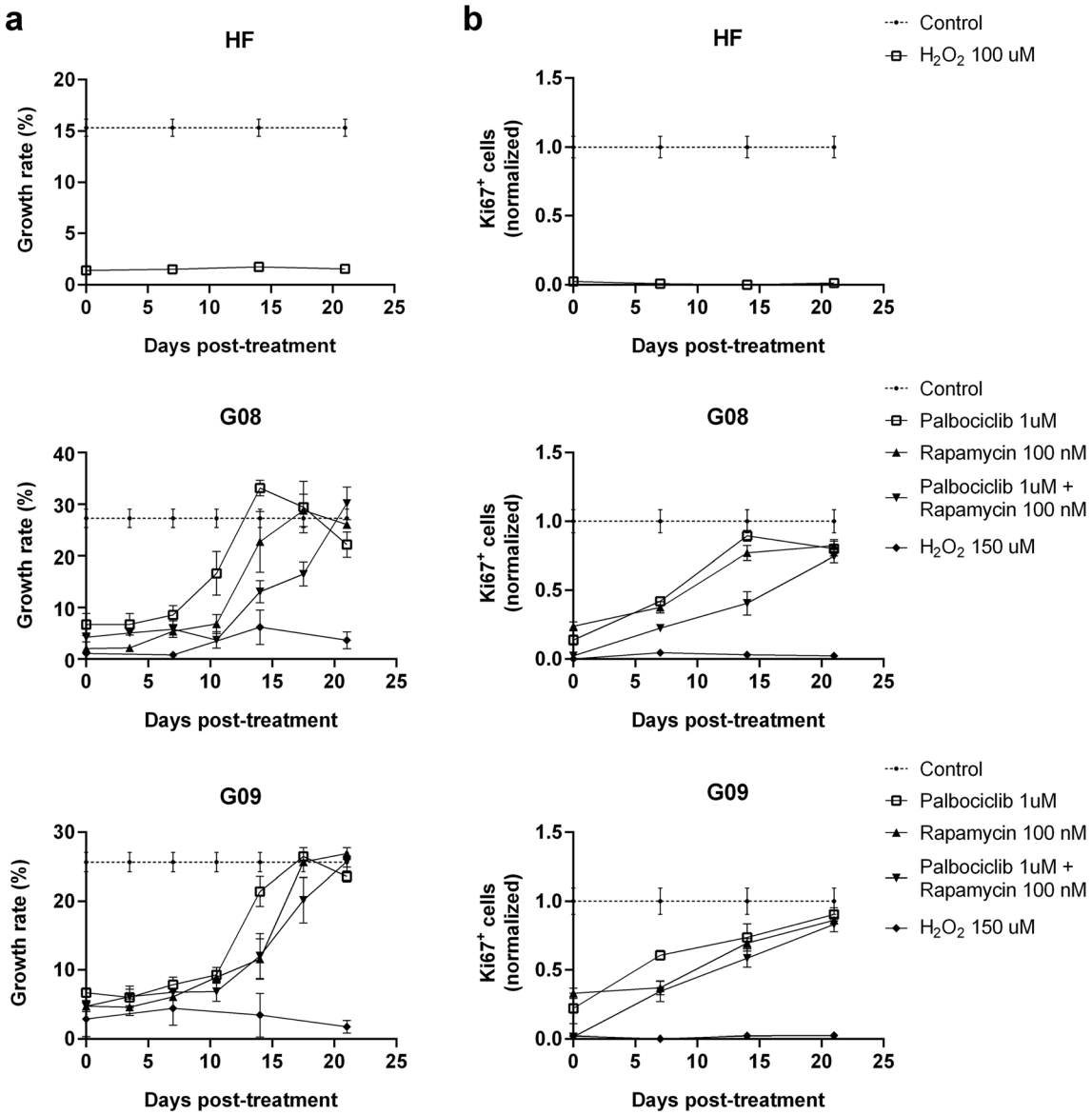

Fig. 6 GSC-ECLs maintain its proliferative potential after a 14-day treatment of Palbociclib, Rapamycin, or a combination of both. **a** Daily growth rate and **b** proportion of Ki67$^+$ cells (normalized to values of untreated cells) were measured at different points after the end of the indicated treatment. Each point represents the mean ± S.E.M. of three independent experiments

treated GSC-ECLs enter into a quiescent state rather than a senescent one. Contrary to our findings, it has been reported that prolonged exposure to Palbociclib in certain cancer cell types induces a permanent loss of proliferative potential [16, 18, 30, 35]. The fact that Palbociclib may have a cell-type specific action, probably associated with each molecular context, could explain these discrepancies. For instance, Kovatcheva et al. described that the glioma cell line SNB19, which expresses a point mutation of p53 (R273H), was able to senesce after prolonged exposure to Palbociclib [16]. Of note, none of our GSC-ECLs harbor this p53 mutation [4]. However, another explanation for these differences could consist in the period after which proliferative potential was assessed. For example, Leontieva et al reported that normal retinal pigment epithelial cells (RPE) and melanoma cells (MEL10) did not resume proliferation by 6 or 7 days after Palbociclib removal respectively [18]. In our study, GSC-ECL did not resume proliferation after the first week of recovery either, but did between 14 and 21 days post-treatment.

Taking into account that Rapamycin reverted the SA-β-gal$^+$ phenotype, we wondered whether this inhibitor would accelerate the recovery of the proliferative capacity of Palbociclib-treated cells. We found that in GSCE-ECLs exposed to the combination of Palbociclib plus Rapamycin, the addition of Rapamycin not only did not accelerate the recovery period, but actually delayed it compared with cells treated with Palbociclib alone. Moreover, in GSC-ECLs exposed to Rapamycin alone, the recovery period was similar to that

observed with Palbociclib. This was surprising considering that Rapamycin did not induce SA-β-gal activity. The fact that the recovery times of GSC-ECLs treated with Rapamycin, with or without Palbociclib, were similar or more extended than those observed in Palbociclib-treated cells reinforces the concept that Palbociclib-treated GSC-ECLs were in a quiescent state rather than in a senescent one.

Finally, we wondered whether the failure of Palbociclib to induce senescence in our GSC-ECLs is due to an intrinsic inability of Palbociclib to induce senescence in certain glioma cell lines or it is due to a general incapacity of these cells to senesce (which could be given, for example, by the absence of $p16^{INK4a}$). So, to evaluate if these cells are able to senesce at all, we exposed them to H_20_2 and found that all tested cell lines entered an irreversible growth arrest concomitantly with a marked increase of SA-β-gal activity and the appearance of a SASP. Thus, herein, we determined that GSC-ECLs are able to enter senescence. Therefore, the identification of proteins controlling the transition from quiescence into senescence in glioma stem cells may help to develop more effective therapies for GBM. Recently, it has been shown that Palbociclib monotherapy is not an effective treatment for recurrent GBM [36]. However, in this study, selected patients were heavily pre-treated and the retinoblastoma (RB) gene status was not evaluated by sequencing techniques. Therefore, the effectiveness of targeting the CDK4/6 pathway in GBM patients with wild type RB in earlier stages of the disease needs to be investigated.

In brief, we found that GSC-ECLs are highly reliant on CDK6 for proliferation and that inhibition of its activity with Palbociclib leads to a transient growth arrest but not to permanent cell cycle exit. Despite this, we found that Palbociclib is very effective at halting glioma stem cell proliferation and thus is not without merit. Therefore, specific CDK6 inhibitors could be used in order to delay tumor progression, prolonging patient survival.

Funding Information This work was supported by the Fundación para la Lucha contra las Enfermedades Neurológicas de la Infancia (FLENI) and Instituto Nacional del Cáncer (INC) de la República Argentina.

References

1. Stupp R, Mason WP, van den Bent MJ, Weller M, Fisher B, Taphoorn MJ, Belanger K, Brandes AA et al (2005) Radiotherapy plus concomitant and adjuvant temozolomide for glioblastoma. N Engl J Med 352(10):987–996
2. Visvader JE, Lindeman GJ (2008) Cancer stem cells in solid tumours: accumulating evidence and unresolved questions. Nat Rev Cancer 8(10):755–768
3. Reya T, Morrison SJ, Clarke MF, Weissman IL (2001) Stem cells, cancer, and cancer stem cells. Nature 414(6859):105–111
4. Videla Richardson GA, Garcia CP, Roisman A, Slavutsky I, Fernandez Espinosa DD, Romorini L, Miriuka SG, Arakaki N et al (2016) Specific preferences in lineage choice and phenotypic plasticity of glioma stem cells under BMP4 and noggin influence. Brain Pathol 26(1):43–61
5. Hunter T, Pines J (1994) Cyclins and cancer. II: cyclin D and CDK inhibitors come of age. Cell 79(4):573–582
6. Sherr CJ (1996) Cancer cell cycles. Science 274(5293):1672–1677
7. van den Heuvel S, Harlow E (1993) Distinct roles for cyclin-dependent kinases in cell cycle control. Science 262(5142):2050–2054
8. Sherr CJ, Roberts JM (1999) CDK inhibitors: positive and negative regulators of G1-phase progression. Genes Dev 13(12):1501–1512
9. Peeper DS, Upton TM, Ladha MH, Neuman E, Zalvide J, Bernards R, DeCaprio JA, Ewen ME (1997) Ras signalling linked to the cell-cycle machinery by the retinoblastoma protein. Nature 386(6621):177–181
10. Parsons DW, Jones S, Zhang X, Lin JC, Leary RJ, Angenendt P, Mankoo P, Carter H et al (2008) An integrated genomic analysis of human glioblastoma multiforme. Science 321(5897):1807–1812
11. Fry DW, Harvey PJ, Keller PR, Elliott WL, Meade M, Trachet E, Albassam M, Zheng X et al (2004) Specific inhibition of cyclin-dependent kinase 4/6 by PD 0332991 and associated antitumor activity in human tumor xenografts. Mol Cancer Ther 3(11):1427–1438
12. Finn RS, Martin M, Rugo HS, Jones S, Im SA, Gelmon K, Harbeck N, Lipatov ON et al (2016) Palbociclib and letrozole in advanced breast cancer. N Engl J Med 375(20):1925–1936
13. Hamilton E, Infante JR (2016) Targeting CDK4/6 in patients with cancer. Cancer Treat Rev 45:129–138
14. Baughn LB, Di Liberto M, Wu K, Toogood PL, Louie T, Gottschalk R, Niesvizky R, Cho H et al (2006) A novel orally active small molecule potently induces G1 arrest in primary myeloma cells and prevents tumor growth by specific inhibition of cyclin-dependent kinase 4/6. Cancer Res 66(15):7661–7667
15. VanArsdale T, Boshoff C, Arndt KT, Abraham RT (2015) Molecular pathways: targeting the cyclin D-CDK4/6 axis for cancer treatment. Clin Cancer Res 21(13):2905–2910
16. Kovatcheva M, Liu DD, Dickson MA, Klein ME, O'Connor R, Wilder FO, Socci ND, Tap WD et al (2015) MDM2 turnover and expression of ATRX determine the choice between quiescence and senescence in response to CDK4 inhibition. Oncotarget 6(10):8226–8243
17. Michaud K, Solomon DA, Oermann E, Kim JS, Zhong WZ, Prados MD, Ozawa T, James CD et al (2010) Pharmacologic inhibition of cyclin-dependent kinases 4 and 6 arrests the growth of glioblastoma multiforme intracranial xenografts. Cancer Res 70(8):3228–3238
18. Leontieva OV, Blagosklonny MV (2013) CDK4/6-inhibiting drug substitutes for p21 and p16 in senescence: duration of cell cycle arrest and MTOR activity determine geroconversion. Cell Cycle 12(18):3063–3069
19. Schmitt CA (2007) Cellular senescence and cancer treatment. Biochim Biophys Acta 1775(1):5–20
20. Garcia CP, Videla Richardson GA, Dimopoulos NA, Fernandez Espinosa DD, Miriuka SG, Sevlever GE, Romorini L, Scassa ME (2016) Human pluripotent stem cells and derived neuroprogenitors display differential degrees of susceptibility to BH3 mimetics ABT-263, WEHI-539 and ABT-199. PLoS One 11(3):e0152607
21. Morris-Hanon O, Furmento VA, Rodriguez-Varela MS, Mucci S, Fernandez-Espinosa DD, Romorini L, Sevlever GE, Scassa ME et al (2017) The cell cycle inhibitors p21(Cip1) and p27(Kip1) control proliferation but enhance DNA damage resistance of glioma stem cells. Neoplasia 19(7):519–529
22. Cicenas J, Kalyan K, Sorokinas A, Stankunas E, Levy J, Meskinyte I, Stankevicius V, Kaupinis A et al (2015) Roscovitine in cancer and other diseases. Ann Transl Med 3(10):135
23. Cicenas J, Valius M (2011) The CDK inhibitors in cancer research and therapy. J Cancer Res Clin Oncol 137(10):1409–1418

24. Anders L, Ke N, Hydbring P, Choi YJ, Widlund HR, Chick JM, Zhai H, Vidal M et al (2011) A systematic screen for CDK4/6 substrates links FOXM1 phosphorylation to senescence suppression in cancer cells. Cancer Cell 20(5):620–634
25. Wang Z, Wei D, Xiao H (2013) Methods of cellular senescence induction using oxidative stress. Methods Mol Biol 1048:135–144. https://doi.org/10.1007/978-1-62703-556-9_11
26. Coppe JP, Desprez PY, Krtolica A, Campisi J (2010) The senescence-associated secretory phenotype: the dark side of tumor suppression. Annu Rev Pathol 5:99–118
27. Tadesse S, Yu M, Kumarasiri M, Le BT, Wang S (2015) Targeting CDK6 in cancer: state of the art and new insights. Cell Cycle 14(20):3220–3230
28. Demidenko ZN, Zubova SG, Bukreeva EI, Pospelov VA, Pospelova TV, Blagosklonny MV (2009) Rapamycin decelerates cellular senescence. Cell Cycle 8(12):1888–1895
29. Nam HY, Han MW, Chang HW, Lee YS, Lee M, Lee HJ, Lee BW, Lee KE et al (2013) Radioresistant cancer cells can be conditioned to enter senescence by mTOR inhibition. Cancer Res 73(14):4267–4277
30. Yoshida A, Lee EK, Diehl JA (2016) Induction of therapeutic senescence in vemurafenib-resistant melanoma by extended inhibition of CDK4/6. Cancer Res 76(10):2990–3002
31. Zou X, Ray D, Aziyu A, Christov K, Boiko AD, Gudkov AV, Kiyokawa H (2002) Cdk4 disruption renders primary mouse cells resistant to oncogenic transformation, leading to Arf/p53-independent senescence. Genes Dev 16(22):2923–2934
32. Bonelli MA, Digiacomo G, Fumarola C, Alfieri R, Quaini F, Falco A, Madeddu D, La Monica S et al (2017) Combined inhibition of CDK4/6 and PI3K/AKT/mTOR pathways induces a synergistic anti-tumor effect in malignant pleural mesothelioma cells. Neoplasia 19(8):637–648
33. Paugh BS, Paugh SW, Bryan L, Kapitonov D, Wilczynska KM, Gopalan SM, Rokita H, Milstien S et al (2008) EGF regulates plasminogen activator inhibitor-1 (PAI-1) by a pathway involving c-Src, PKCdelta, and sphingosine kinase 1 in glioblastoma cells. FASEB J 22(2):455–465
34. Piperi C, Samaras V, Levidou G, Kavantzas N, Boviatsis E, Petraki K, Grivas A, Barbatis C et al (2011) Prognostic significance of IL-8-STAT-3 pathway in astrocytomas: correlation with IL-6, VEGF and microvessel morphometry. Cytokine 55(3):387–395
35. Valenzuela CA, Vargas L, Martinez V, Bravo S, Brown NE (2017) Palbociclib-induced autophagy and senescence in gastric cancer cells. Exp Cell Res 360(2):390–396
36. Taylor JW, Parikh M, Phillips JJ, James CD, Molinaro AM, Butowski NA, Clarke JL, Oberheim-Bush NA et al (2018) Phase-2 trial of palbociclib in adult patients with recurrent RB1-positive glioblastoma. J Neuro-Oncol 140(2):477–483